Sulfur compounds characterization using FT-ICR MS: Towards a better comprehension of vacuum gas oils hydrodesulfurization process

Julie Guillemant, Alexandra Berlioz-Barbier, Fabien Chainet, Luis de Oliveira, Marion Lacoue-Nègre, Jean-François Joly, Ludovic Duponchel

Sulfur compounds characterization using FT-ICR MS: towards a better comprehension of vacuum gas oils hydrodesulfurization process

Julie Guillemant[1], Alexandra Berlioz-Barbier*[1], Fabien Chainet[1], Luis P. de Oliveira[1], Marion Lacoue-Nègre[1], Jean-François Joly[1], and Ludovic Duponchel[2]

[1] IFP Energies nouvelles, Rond-Point de l'Echangeur de Solaize, BP 3 - 69360 Solaize, France

[2] Univ. Lille, CNRS, UMR 8516 - LASIRE – Laboratoire avancé de spectroscopie pour les interactions, la réactivité et l'environnement, F-59000 Lille, France

Corresponding Author: Alexandra Berlioz-Barbier (alexandra.berlioz-barbier@ifpen.fr)

Abstract

Some aromatic sulfur compounds contained in vacuum gas oils are known to be very refractory to hydrotreatment. Thus, a better knowledge of these molecules would help to improve hydrodesulfurization efficiency by designing targeted catalysts or choosing adequate operating conditions for hydrotreatment process. The characterization of such compounds using advanced analytical techniques such as Fourier Transform Ion Cyclotron Resonance Mass Spectrometry (FT-ICR MS) can give more information about the aromaticity and the number of carbon atoms of these refractory molecules. One vacuum gas oil feed and six hydrotreated samples obtained from pilot plant tests at several temperatures or using different catalysts have been analyzed using APPI(+)-FT-ICR MS. The differences of the aromaticity and number of carbon atoms among the several hydrotreated samples have been investigated to to identify the effects of catalysts and temperatures over hydrotreatment process. Principal Component Analysis was used to explore the obtained data and put forward the variables explaining most of the variance between the hydrotreated samples.

Keywords: Vacuum gas oils ; hydrodesulfurization ; catalysis ; sulfur compounds ; mass spectrometry ; chemometrics

1. Introduction

As environmental specifications become more and more severe regarding sulfur compounds, refiners need to improve hydrodesulfurization processes to reduce as much as possible the sulfur content to less than 10 ppm in commercial on-road gas oils[1,2]. Such gas oils (GO) are mainly obtained through conversion processes such as Fluid Catalytic Cracking (FCC) or Hydrocracking (HCK) from heavier cuts such as vacuum gas oils (VGO) whose sulfur content are very high. Thus, a first hydrotreatment step is often introduced before conversion processes to improve the quality of the heavy cut (i.e.,VGO) before conversion into gas oil cut. However, some sulfur compounds contained in vacuum gas oils are refractory to hydrotreatment and there is no analytical method providing both quantitative and qualitative results to feed hydrotreatment models to improve such process[3–5]. Moreover, such method would also be helpful to perform catalysts screening, to go further into desulfurization mechanism comprehension as described for lighter cuts such as gasoline as well as optimizing modeling processes[6,7].

Two-dimensional comprehensive gas chromatography (GC×GC) coupled to Sulfur Chemiluminescence Detector (SCD) is mainly used to characterize sulfur compounds in gas oil samples[8,9]. However, GC×GC analysis does not allow the analysis of polar compounds in vacuum gas oils samples as the polar compounds are not fully resolved thus preventing their quantification [10].

Within a mass spectrometry context, sulfur compounds are rather identified as apolar compounds. [11–15]. Two ionization sources are mainly available for sulfur compounds characterization: atmospheric pressure photo-ionization (APPI) and methylation of sulfur compounds followed by electrospray ionization (Me-ESI). Me-ESI is more sensitive towards low alkylated compounds whereas APPI ionizes a broader range of aromatic compounds[16,17]. Thus, APPI ionization source is preferred rather than Me-ESI to perform VGO analysis as very aromatic compounds found in the VGO feedstock used to produce the hydrotreated samples might not be efficiently ionized using Me-ESI without any pre-fractionation of the vacuum gas oils[17].

Chemometric tools have been proved to be efficient to extract significant variables among large FT-ICR MS datasets, especially Principal Component Analysis (PCA)[18–20]. The use of

such tools is then particularly suited to look for reactivity descriptors that could explain the differences observed between several hydrotreated samples [21]. When vacuum gas oils matrices that are more complex than gas oils matrices are considered, the number of significant variables is even increased hence proving the interest of such methods [22,23].

This paper presents the APPI(+)-FT-ICR MS analysis of one vacuum gas oil feed and six hydrotreated samples obtained from catalytic tests at several temperatures and with two different catalysts. The pseudo-concentrations of each family have been followed throughout hydrotreatment process for a better understanding of removal mechanisms throughout the present hydrotreatment operating conditions. Finally, PCA was applied on data obtained for the feed and the hydrotreated samples to explore the generated dataset.

2. Material and Methods

2.1. Vacuum gas oils

6 hydrotreated samples with different hydrodesulfurization (HDS) levels have been selected for this study. The samples have been produced from hydrotreating pilot tests of a VGO feedstock over two different catalysts (A) and (B). The different levels of HDS have been obtained by varying the reactor temperature while keeping the other operating conditions such as reactor pressure, LHSV, H_2/oil ratio) constant. The S content was determined by wavelength dispersive X-rays fluorescence (WDXRF) using a Panalytical Axios (Almelo, Netherlands) 4 kW equipped with a Cr anode. 2 mL of the solution was introduced within a cup with a Mylar 6 µm film according to an IFPEN internal method. Details about the chosen samples are given in Table 1. All samples have been first solubilized in toluene to 1% w/w and further diluted in a 75%-25% Toluene-Methanol solution to 0.05% v/v for FT-ICR MS analysis.

Table 1. Vacuum gas oil samples characteristics

Sample	Reactor Temperature	Sulfur content (ppm)	Boiling Point Ranges (°C)	Catalyst
Feed (85% Arabian Light + 15% Irak)	-	18921	394-580	-
A-1	Low temperature (1)	1251		A
A-2	Middle temperature (2)	693		A
A-3	High temperature (3)	334		A
B-1	Low temperature (1)	949		B
B-2	Middle temperature (2)	483		B
B-3	High temperature (3)	200		B

2.2. FT-ICR MS analysis

VGO samples were analyzed in APPI(+)-FT-ICR MS considering 6 technical replicates to assess the ionization repeatability of the analysis. Mass spectrometry (MS) analyses were performed using a LTQ FT Ultra Fourier Transform Ion Cyclotron Resonance Mass Spectrometer (FT-ICR MS) (ThermoFisher Scientific, Bremen Germany) equipped with a 7T magnet (Oxford Instruments) and with APPI source (Syagen Technology, Tustin CA, USA) used in positive mode. Mass range was set to *m/z* 98-1000. 4 µ-scans, 70 scans and an initial resolution set to 200,000 (transient length of 1.6s) at *m/z*=500 (center of average vacuum gas oil mass distribution) were recorded for each sample. Transient signal was recorded to enable further data processing. Tube lens, capillary voltage and vaporization temperature were fixed to 70 V, 30 V and 250°C respectively. Sheath gas was 20 a.u. and auxiliary gas was 5 a.u.. Nitrogen was used in both cases. External mass calibration was performed using a home-made sodium formiate clusters solution (sodium formate from VWR, Fontenay-sous-Bois, France) from about 90 Da to 1000 Da.

2.3. Spectral data processing

Spectral data were processed using several softwares. More details about full data processing are available elsewhere[24] leading to a resolution of about 445,000 at *m/z* 498 sufficient to resolve the 3.4 mDa difference between C_3 and SH_4. Molecular formula assignment conditions were the following ones: $C_{0\text{-}100}H_{0\text{-}200}O_{0\text{-}5}N_{0\text{-}5}S_{0\text{-}5}$ with maximum content of heteroatoms of 5 for the vacuum gas oils samples. The error between the theoretical and experimental masses was set to 1 ppm after iterative mass recalibration based on S1 family (most abundant family)[25]. S1 family corresponds to radicalar ions and was supposed to contain all elementary sulfur as only a small percentage of protonated cations were observed and they would be more likely to correspond to fragments rather than precursors Relative intensities were calculated by multiplying the compound absolute intensity by 100 and divided by the sum of all S1 absolute intensities. Pseudo-concentrations in sulfur were obtained by multiplying relative intensities by the amount of sulfur in the sample. Families were attributed regarding values of Double Bond Equivalent (DBE) with DBE = c - h/2 + n/2 + 1 where c corresponds to the number of carbon atoms, h to the number of hydrogen atoms and n to the number of nitrogen atoms. As FT-ICR MS does not

allow isomers identification, the types of structures most likely to correspond to molecules with the indicated DBE are available in Table 2 [17,26].

Table 2. Types of sulfur compounds found in crude oils and their corresponding DBE.

Thiols DBE 1-2	Thiophenes (T) DBE 3-4-5	Benzothiophenes (BT) DBE 6-7-8	Dibenzothiophenes (DBT) DBE 9-10-11	Naphtobenzothiophenes (NBT) DBE 12-13-14
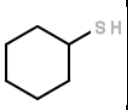		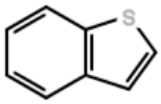	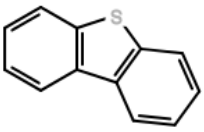	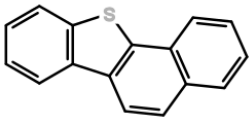

2.4.Principal Component Analysis

As this study focuses on sulfur compounds contained in VGO, only molecular formulas containing a single atom of sulfur were taken into account for spectral analysis. The six different replicates were used as single samples to assess the repeatability of the FT-ICR MS analysis through PCA. The data formatting has been described and successfully applied on gas oil matrices elsewhere[21] and adapted here to VGO data. Briefly, APPI-FT-ICR MS data was re-arranged into a 42×2500 matrix where 42 correspond to the 7 samples times 6 replicates and 2500 to the possible combinations of DBE (from 1 to 25) and carbon number (from 1 to 100). The relative intensities of the peaks have been considered as variables and the matrix has been mean-centered prior to statistical analysis.

All models were developed with the PLS_Toolbox version 8.6 for Matlab version R2018b (Eigenvector Research Inc, Wenatchee, WA, USA). Replicates from sample A-3 were used for validation and all other samples were used for performing PCA. The optimization of the model was performed with venitian-blinds cross-validation (10 data splits, 20 samples per blind, 20 maximum principal components). Optimal number of components for PCA was chosen based on % explained cumulative variance and log(eigenvalues) values.

3. Results and Discussion

3.1. Global vacuum gas oils analysis

After hydrotreatment, only HC, N1 Ox and S1 compounds are found in the hydrotreatment samples (see Figure S1 in Supporting Information) both in radicalar $M^{+\cdot}$ and protonated $[M+H]^+$) forms. A small proportion of disulfur compounds has been identified in the feedstock but no disulfur compounds have been identified in the hydrotreated samples meaning that the disulfur compounds have been removed during hydrotreatment and thus are not considered in this study. The plots of DBE as a function of the carbon number for the 7 samples (Feed and hydrotreated products) are very useful to get a quick overview of the effects of both catalysts and temperatures. Indeed, as seen in Figure 1, the rise of temperature (Low, Middle and High temperature) is directly linked to the decrease of identified S1 compounds which is in accordance with expected behavior. The relative abundance of the S1 class also decreases accordingly to the sulfur content in the sample, as seen in Figure S1 in Supporting Information. The specificities of each catalyst are also highlighted as profiles obtained are different for a given temperature.

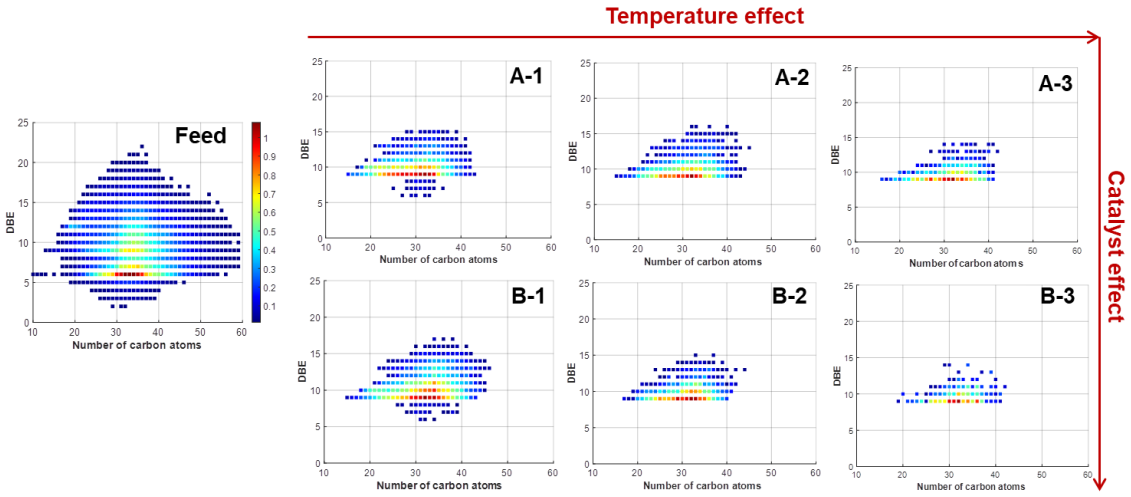

Fig. 1. Comparison of obtained DBE=f(#C) diagrams for the feed and the six hydrotreated samples (A-1 to B-3) for the class S1.

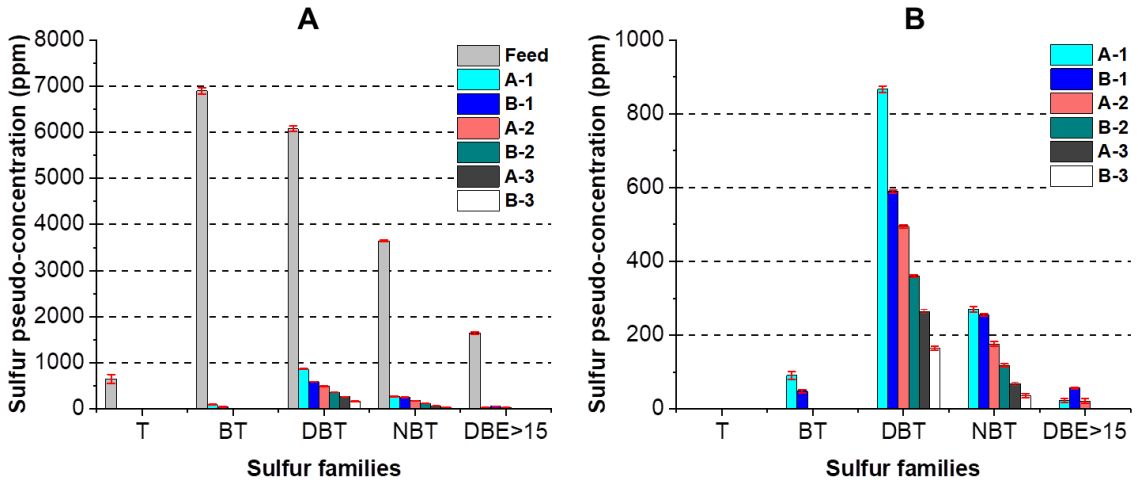

195

196 **Fig.2. (A) Comparison of sulfur families identified for the feed and its hydrotreated**
197 **samples. (B) Zoom over the hydrotreated samples.**

198 A large range of sulfur families is observed in Feed sample with mainly benzothiophenes (BT)
199 and dibenzothiophenes (DBT), as shown in Figure 2A. In the hydrotreated samples, a sharp
200 decrease is observed for most of sulfur families, visible in Figure 2B. This is obvious for BT
201 whose concentrations are close to zero at highest HDS conversion level revealing the high
202 reactivity of these compounds. Naphtobenzothiophenes (NBT) and especially dibenzothiophenes
203 (DBT) are the main remaining families within the most severely hydrotreated sample (B-3)..
204 Their refractory character is well known in the literature[1,3,4]. The reactor temperature effect is
205 also observed with gradual decreasing of pseudo-concentrations as the temperature rises.
206 Regarding the catalysts, catalyst B is more efficient than catalyst A in removing the BT and
207 DBT compounds. For the HDS of NBT family, no obvious difference is observed between both
208 catalysts indicating that for a given low temperature catalyst B is not more efficient than catalyst
209 A to hydrogenate NBT compounds. This reversal of efficiency might could be related to a
210 possible difference in apparent activation energy on the HDS of the NBT compounds. The
211 activation energy might be lower for catalyst A than for catalyst B, which could be characteristic
212 of two different reaction pathways.

213 To go further, differences regarding aromaticity or number of carbon atoms of the samples have
214 been investigated.

215

3.2.Aromaticity changes.

The aromaticity changes within each sulfur family have also been studied by comparing the pseudo-concentrations for several DBE within the same family, as shown in Figure 3. The compounds remaining in the most hydrotreated samples (*i.e* A-3 and B-3) have DBE values contained between 9 and 14. Again, the gradual decrease of the pseudo-concentrations is observed according to the reactor temperature and the higher efficiency of the catalyst B is spotted for moderate and high temperatures. The most intense aromaticity degree in the most severely hydrotreated sample corresponds to a DBE equal to 9 which could correspond to the classical backbone DBT molecule or to a benzothiophene core with three additional naphtenic rings.

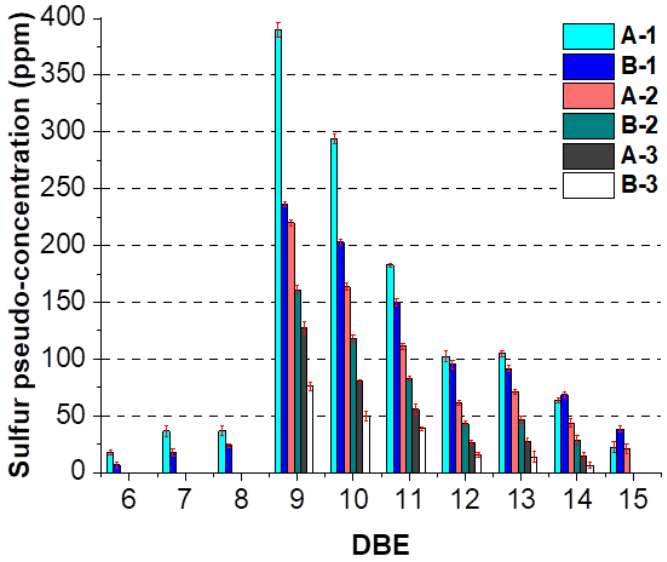

Fig. 3. Evolutions of sulfur pseudo-concentrations as a function of aromaticity degree (DBE) for the several hydrotreated samples.

For every sulfur family considered, the HDS conversion depends on the aromaticity degree, as shown in the Figure 4. The HDS conversion for each DBE were calculated based on the pseudo-concentrations remaining in the hydrotreated samples compared to the pseudo-concentration observed within the feed. For DBT family (Figure 4A), the HDS conversion of the compounds with a DBE equal to 9 seem to be less converted than other more aromatic DBT compounds and might be potentially more refractory. This result is especially interesting for DBT family as previous observations reported the very refractory character of DBT with DBE equal to 9 also observed for gas oil matrix as well as for vacuum gas oil matrix[21,23].

However, the impact of the aromaticity on the reactivity is also dependent of the catalyst. For the hydrotreated sample B-1, the DBT with DBE equal to 9 and 10 have similar reactivity, while the reactivity of these compounds in the hydrotreated sample A-1 is different. The same behavior is observed in the DBT compounds with DBE 10 and 11 for the hydrotreated samples A-3 and B-3.

As regards NBT, compounds with DBE equal to 13 are more intense than others NBT (DBE 12 and DBE 14), as seen in Figure 4B. This means that the addition of a naphthenic cycle over NBT molecule could decrease the hydrodesulfurization efficiency which was not observed for DBT family. Moreover, species with higher DBE (DBE 14, 15, 16...) could also be partially hydrogenated during hydrodesulfurization and would enrich the content in DBE 13.

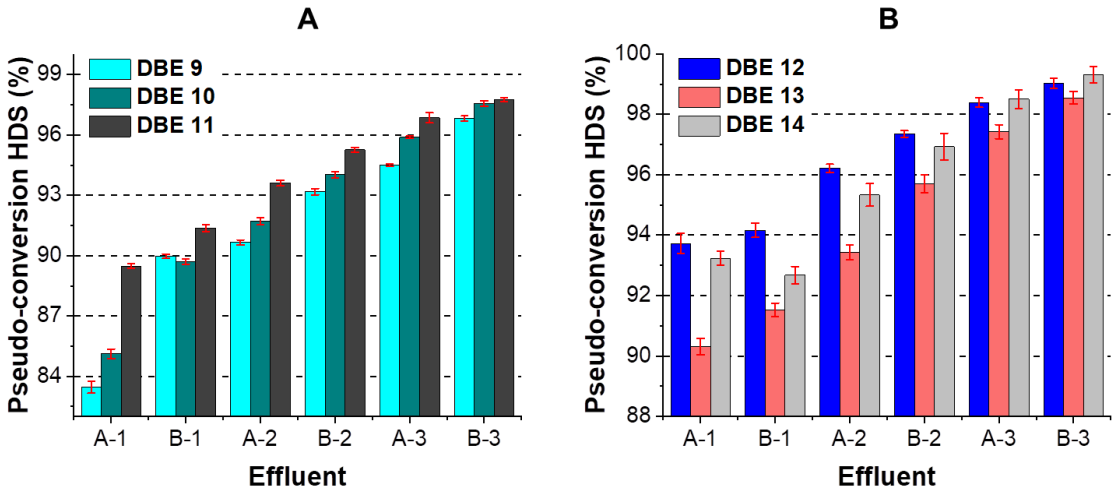

Fig. 4. (A) Evolution of the HDS conversion percentage of the different hydrotreated samples as a function of DBE 9-11. (B) Evolution of the HDS conversion percentage of the different hydrotreated samples as a function of DBE 12-14.

The samples obtained at low temperature (A1-B1) seem to have a different catalytic behavior according to sulfur families, as seen in Figure 5. The HDS of benzothiophenes compounds, (DBE between 6 and 8) is similar for both catalysts, while the catalyst B is more active (i.e more selective) than catalyst A on the HDS of the DBT compounds (DBE between 9 and 11). The activity of the catalysts become similar again between DBE 12 and 13. Finally, a selectivity inversion is observed with catalyst A being more active than catalyst B for the compounds with DBE between 14 and 16. Thus, catalyst B is globally more selective towards dibenzothiophenes

(DBE 9-10-11) than catalyst A but surprisingly less efficient for more aromatic compounds such as naphtobenzothiophenes (DBE 14-16). This behavior might be linked to a difference in activation energy between both catalysts as explained in the section 3.1.

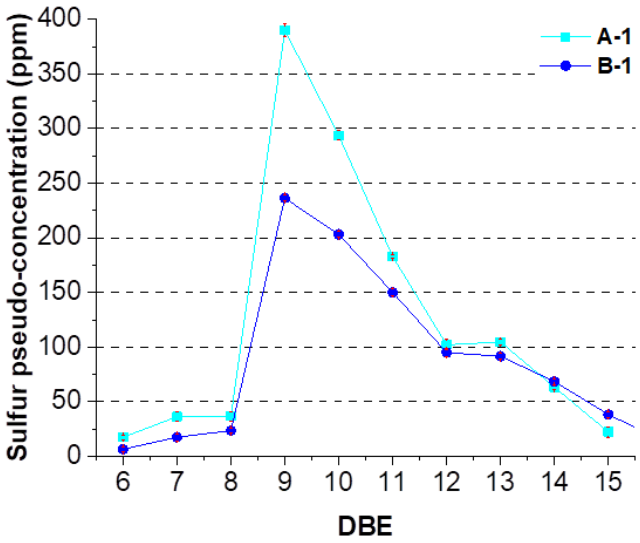

Fig.5. Evolution of the sulfur pseudo-concentration as a function of DBE for the effluents A-1 and B-1.

Moreover, a potential hydrogenation competition between hydrocarbons and sulfur might be suspected within the reactor [27] and especially within samples A-1 and B-1. To evaluate this, the evolution of the DBE and number of carbon atoms of the hydrocarbons compounds (HC class) in these effluents has been plotted in Figure 6. The evolution of the corresponding DBE=f(#C) plots for this class from all effluents are also available in Figure S2 in Supporting Information. A clear shift of the sample A-1 is spotted compared to the sample B-1 in terms of aromaticity as well as number of carbon atoms. Especially, the sample A-1 should undergoes more hydrogenation reactions as its relative intensities in poorly aromatic compounds (DBE < 9) are higher than those observed for sample B-1. Moreover, as the alkylation range remains similar between the feed and its effluents, the shift in alkylation observed for the hydrotreated samples can be attributed to a reactivity difference between the "poorly" (< C40) and very alkylated species (> C40). To go further, an appropriate kinetic study should be performed to fully explain and understand the hydrogenation competitions between sulfur and hydrocarbons.

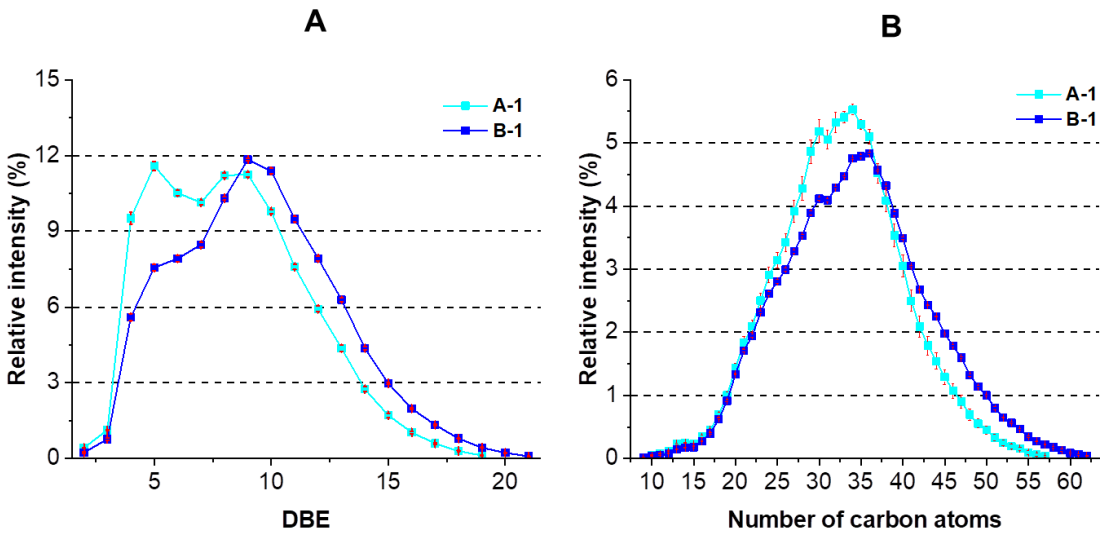

Fig. 6. Evolution of the relative intensity as a function of (A) DBE and (B) number of carbon atoms for samples A-1 and B-1 for the class HC.

3.3. Number of carbon atoms changes

The evolutions of the pseudo-concentrations as a function of the number of carbon atoms of the samples give complementary information. The specific distribution of carbon atoms for DBT with a DBE equal to 9 has been plotted only for hydrotreated samples in Figure 7A. The number of carbon atoms range within refractory compounds have been identified is comprised between 15 and 46.

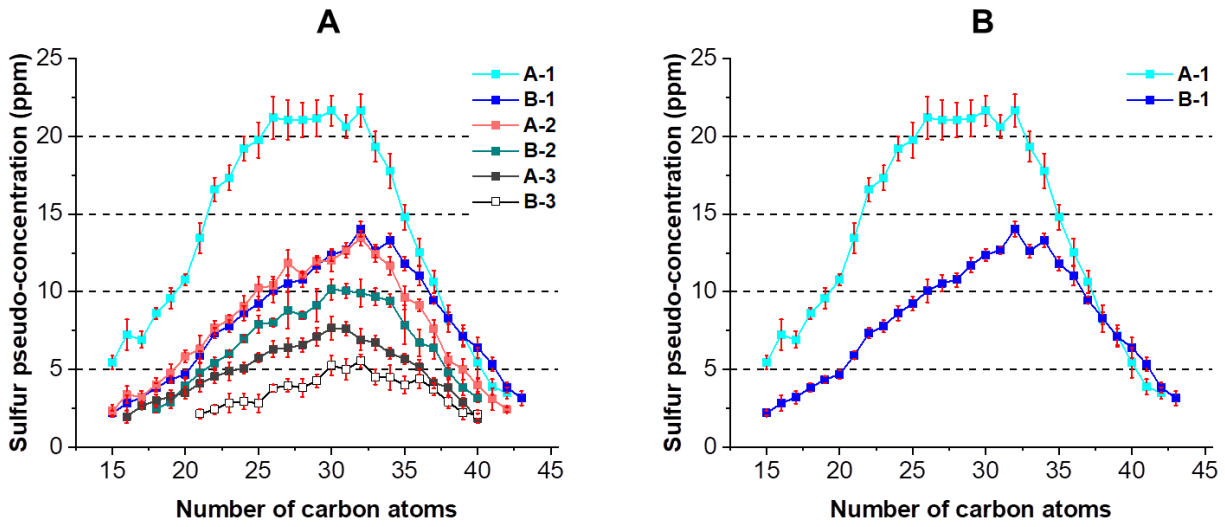

Fig. 7. (A) Evolutions of sulfur pseudo-concentrations as a function of number of carbon atoms of the molecules for DBT molecules with a DBE equal to 9 for the hydrotreated samples A-1 to B-3. (B) Zoomed for A-1 and B-1.

When increasing hydrotreatment conditions, the carbon number distribution has a smaller range and starts from C21 for the most hydrotreated sample (i.e, B-3). This shows that using such catalytic conditions enables the hydrotreatment of less alkylated DBT when moderate conditions do not. Globally, the refractory compounds are most intense around C30 to C35 which is a relatively high degree of alkylation.

The distribution of DBE 9 for the less hydrotreated sample A-1 is shifted to a smaller number of carbon atoms compared to the distribution of sample B-1, as seen in Figure 6B. Thus, dibenzothiophenes in A-1 are less alkylated than dibenzothiophenes analyzed in B-1. As mentioned before, two different desulfurization mechanisms are suspected according to the catalyst considered for low reactor temperature. At low temperature, the catalyst A is more efficient to remove very alkylated compounds while the catalyst B is more efficient towards less alkylated compounds. This trend disappears when increasing the operating temperature hence homogenizing the catalysts efficiency.

It can be mentioned that according to the distribution of the other hydrotreated samples (i.e A-2, B-2, A-3 and B-3), only dehydrodesulfurization may take place with both catalysts at moderate or high reactor temperature.

In summary, sulfur compounds with DBE equal to 9 and carbon atoms number starting from C21 to C42 seem to be the most refractory compounds found for the most severe hydrotreatment operating conditions. To go further, Principal Component Analysis (PCA) was applied on this spectral dataset to extract more information on these samples.

3.4. Principal Component Analysis

PCA was applied on this spectral dataset, also considering only sulfur compounds (S1 class). Moreover, a second statistical analysis has been performed including not only the S1 compounds but also the HC compounds. This analysis showed that the sulfur compounds explain most of the variance between samples and that the hydrocarbons composition does not allow discriminating the different samples whereas it is the most abundant class, hence highlighting the interest of studying the S1 compounds. This second analysis is available in Figure S3 in Supporting Information. Considering the relatively small amount of samples available, only the sample A-3 (corresponding to six replicates) has been used as a validation set and all other samples have been used for calibration. 2 Principal Components (PCs) have been considered in the model leading to a total explained variance of 76%. One replicate from B-3 has been excluded from the model because the relatively high analytical variance between the six replicates distorted the statistical analysis. The score plot obtained over PC1 and PC2 is shown in Figure 7A.

Globally, the different replicates are close to each other for a given sample, except for B-3 for which replicates are a little bit more far away from each other. This can be explained by a decreased analysis sensitivity towards very hydrotreated samples. Validation sample (i.e, A-3) is logically projected between B-2 and B-3 which are the closest samples to A-3 in terms of hydrotreatment severity. A separation between the feed and the different effluents is observed along PC1. It is interesting to note that the increase of HDT severity is visible towards a negative translation over PC2. Moreover, sample B-1 is shifted from the translation over PC1 compared to all other samples, indicated in cyan circle. As seen previously, sample B-1 is the only sample for which a catalyst selectivity inversion is observed for a given reactor temperature. The projection of this sample over PC1 and PC2 confirms its unique behavior.

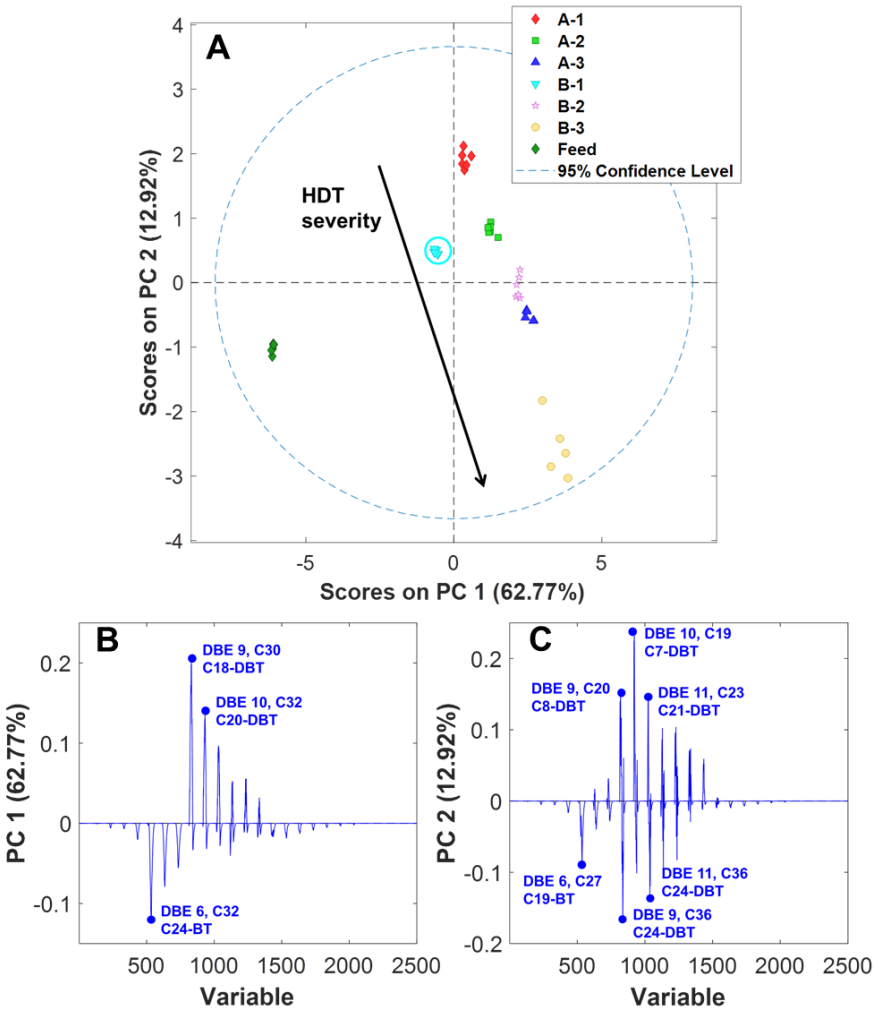

Fig.7. (A) Score plot obtained over PC1 and PC2 for the feed and its hydrotreated samples. (B) Loadings plot obtained for PC1. (C) Loadings plot obtained for PC2.

The loadings plots correspond to the visualization of the distribution of the variables over several principal components. Those obtained from the first and second principal components are shown in Figures 7B and 7C. When considering PC1, three variables are mainly expressed: C4+-BT (corresponding to a benzothiophene core with 24 additional carbon atoms with a DBE equal to 6) and two C4+-DBT (dibenzothiophenes cores with respectively 18 and 20 additional carbon atoms and DBE equal to 9 and 10). The C4+-BT variable is negatively expressed over PC1 when both C4+-DBT variables are positively expressed. Thus, the negative projection of the feed along PC1 is due to its relative intensity of benzothiophenes which is lower than the ones observed for the different effluents except for the sample A-1 which also explains its atypical character. This is in agreement with the previous observations stating that the benzothiophenes are totally

removed in effluents obtained at moderate or high reactor temperatures (i.e, A-2, B-2, A-3 and B-3) as they are easily converted when performing hydrodesulfurization[4]. On the opposite, the positive projection of the hydrotreated samples is mainly due to the major presence of dibenzothiophenes with several aromaticity levels (DBE 9 and DBE 10). Again, this is consistent with previous observations putting forward the very refractory character of these compounds. As regards PC2, very alkylated variables are negatively expressed with DBE equal to 6, 9 and 11 when less alkylated variables are positively expressed with DBE equal to 9, 10 and 11. The expression of C_{4+}-BT is due to the negative projection of the feed along PC2. It is worth noticing that for DBE 9 and 11 the distributions of the number of carbon atoms are splitted into both positive and negative contributions, showing the subtle discriminative power of PCA. Thus, the increase of HDS severity goes with a raise of alkylation levels for given DBEs meaning that very poly-alkylated dibenzothiophenes are more refractory than lower alkylated ones. This also confirms the difference of selectivity for DBE 9 observed for catalysts A and B at low temperature which is actually due to alkylation degree shifts with catalyst A leading to less alkylated products and catalyst B leading to more alkylated products. As the other principal components (PC3, PC4, PC5...) did not allow extracting more information, they are not discussed here.

4. Conclusion

The relevance of FT-ICR MS as a pseudo-quantitative tool for the hydrotreatment monitoring of vacuum gas oils has been assessed in this paper by comparing the pseudo-concentrations obtained for one feed and its six hydrotreated samples. A comprehensive study of the effect of temperature and catalyst over hydrotreatment process has been done. This helped us to highlight some refractory compounds in vacuum gas oil hydrotreatment and it can be mentioned that these compounds have already been found to be problematic for gas oil hydrotreatment. This indicates that no matter the fact that much more aromatic and alkylated compounds can be found in VGO, dibenzothiophenes and their derivates with low aromatic content are most likely to be the most problematic compounds in HDT, followed by naphtobenzothiophenes and their derivatives. Especially, the study of aromaticity and alkylation levels gave some clues on the most refractory aromatic levels that are DBE 9 for the dibenzothiophenes family and DBE 12 for the naphtobenzothiophenes family. The number of carbon atoms of these refractory molecules has also been described, coming from C21 to C42 which relates to very alkylated molecules as the DBT aromatic core molecule only contains 12 carbon atoms. The application of chemometric tool such as PCA confirmed all the previous observations and helped in the identification of key variables explaining some selectivity differences between both catalysts at low temperature. In summary, dibenzothiophenes with high number of carbon atoms and DBE equal to 9 are revealed to be the main remaining species in VGO hydrotreatment process. Thus, specific catalysts could be designed to target these molecules and improve HDT efficiency. Moreover, other techniques could be applied such as ion mobility to identify the most refractory isomers in more severely hydrotreated samples and also to identify the nature of the carbon substituents on these molecules.

5. References

[1] A. Ishihara, D. Wang, F. Dumeignil, H. Amano, E.W. Qian, T. Kabe, Oxidative desulfurization and denitrogenation of a light gas oil using an oxidation/adsorption continuous flow process, Applied Catalysis A: General 279 (2005) 279–287.

[2] V. Rabarihoela-Rakotovao, F. Diehl, S. Brunet, Deep HDS of Diesel Fuel: Inhibiting Effect of Nitrogen Compounds on the Transformation of the Refractory 4,6-Dimethyldibenzothiophene Over a NiMoP/Al2O3 Catalyst, Catal Lett 129 (2009) 50–60.

[3] M. Liu, M. Wang, L. Zhang, Z. Xu, Y. Chen, X. Guo, S. Zhao, Transformation of Sulfur Compounds in the Hydrotreatment of Supercritical Fluid Extraction Subfractions of Saudi Arabia Atmospheric Residua, Energy Fuels 29 (2015) 702–710.

[4] X. Ma, K. Sakanishi, I. Mochida, Hydrodesulfurization Reactivities of Various Sulfur Compounds in Vacuum Gas Oil, Ind. Eng. Chem. Res. 35 (1996) 2487–2494.

[5] D. Valencia, I. García-Cruz, V.H. Uc, L.F. Ramírez-Verduzco, J. Aburto, Refractory Character of 4,6-Dialkyldibenzothiophenes: Structural and Electronic Instabilities Reign Deep Hydrodesulfurization, ChemistrySelect 3 (2018) 8849–8856.

[6] A.S. dos Santos, E. Girard, P. Leflaive, S. Brunet, Competitive adsorptions between thiophenic compounds over a CoMoS/Al2O3 catalyst under deep HDS of FCC gasoline, Applied Catalysis A: General 570 (2019) 292–298.

[7] P. Agarwal, M. Sahasrabudhe, S. Khandalkar, C. Saravanan, M.T. Klein, Molecular-Level Kinetic Modeling of a Real Vacuum Gas Oil Hydroprocessing Refinery System, Energy Fuels 33 (2019) 10143–10158.

[8] C. Lorentz, D. Laurenti, J.L. Zotin, C. Geantet, Comprehensive GC × GC chromatography for the characterization of sulfur compound in fuels: A review, Catalysis Today 292 (2017) 26–37.

[9] F. Adam, H. Muller, A. Al-Hajji, A. Bourane, O. Koseoglu, Oxidative Desulfurization Process Monitoring Using Comprehensive Two-Dimensional Gas Chromatography and Fourier Transform Ion Cyclotron Resonance Mass Spectrometry, Energy Fuels 29 (2015) 2312–2318.

[10] L. Boursier, V. Souchon, C. Dartiguelongue, J. Ponthus, M. Courtiade, D. Thiébaut, Complete elution of vacuum gas oil resins by comprehensive high-temperature two-dimensional gas chromatography, Journal of chromatography. A 1280 (2013) 98–103.

[11] L. Liu, C. Song, S. Tian, Q. Zhang, X. Cai, Y. Liu, Z. Liu, W. Wang, Structural characterization of sulfur-containing aromatic compounds in heavy oils by FT-ICR mass spectrometry with a narrow isolation window, Fuel 240 (2019) 40–48.

[12] A.G. Marshall, R.P. Rodgers, Petroleomics: The next grand challenge for chemical analysis, Accounts of chemical research 37 (2004) 53–59.

[13] A.M. McKenna, J.M. Purcell, R.P. Rodgers, A.G. Marshall, Heavy Petroleum Composition. 1. Exhaustive Compositional Analysis of Athabasca Bitumen HVGO Distillates by Fourier Transform Ion Cyclotron Resonance Mass Spectrometry: A Definitive Test of the Boduszynski Model, Energy Fuels 24 (2010) 2929–2938.

[14] J.M. Purcell, C.L. Hendrickson, R.P. Rodgers, A.G. Marshall, Atmospheric pressure photoionization fourier transform ion cyclotron resonance mass spectrometry for complex mixture analysis, Analytical chemistry 78 (2006) 5906–5912.

[15] D.C. Palacio Lozano, R. Gavard, J.P. Arenas-Diaz, M.J. Thomas, D.D. Stranz, E. Mejía-Ospino, A. Guzman, S.E.F. Spencer, D. Rossell, M.P. Barrow, Pushing the analytical limits:

New insights into complex mixtures using mass spectra segments of constant ultrahigh resolving power, Chemical science 10 (2019) 6966–6978.
[16] J.M. Purcell, P. Juyal, D.-G. Kim, R.P. Rodgers, C.L. Hendrickson, A.G. Marshall, Sulfur Speciation in Petroleum: Atmospheric Pressure Photoionization or Chemical Derivatization and Electrospray Ionization Fourier Transform Ion Cyclotron Resonance Mass Spectrometry, Energy Fuels 21 (2007) 2869–2874.
[17] H. Müller, J.T. Andersson, W. Schrader, Characterization of high-molecular-weight sulfur-containing aromatics in vacuum residues using Fourier transform ion cyclotron resonance mass spectrometry, Analytical chemistry 77 (2005) 2536–2543.
[18] M. Hur, I. Yeo, E. Park, Y.H. Kim, J. Yoo, E. Kim, M.-h. No, J. Koh, S. Kim, Combination of statistical methods and Fourier transform ion cyclotron resonance mass spectrometry for more comprehensive, molecular-level interpretations of petroleum samples, Analytical chemistry 82 (2010) 211–218.
[19] M. Witt, W. Timm, Determination of Simulated Crude Oil Mixtures from the North Sea Using Atmospheric Pressure Photoionization Coupled to Fourier Transform Ion Cyclotron Resonance Mass Spectrometry, Energy Fuels 30 (2015) 3707–3713.
[20] Y.E. Corilo, D.C. Podgorski, A.M. McKenna, K.L. Lemkau, C.M. Reddy, A.G. Marshall, R.P. Rodgers, Oil spill source identification by principal component analysis of electrospray ionization Fourier transform ion cyclotron resonance mass spectra, Analytical chemistry 85 (2013) 9064–9069.
[21] J. Guillemant, F. Albrieux, M. Lacoue-Nègre, L. Pereira de Oliveira, J.-F. Joly, L. Duponchel, Chemometric Exploration of APPI(+)-FT-ICR MS Data Sets for a Comprehensive Study of Aromatic Sulfur Compounds in Gas Oils, Analytical chemistry 91 (2019) 11785–11793.
[22] J. Guillemant, A. Berlioz-Barbier, F. Albrieux, L.P. de Oliveira, M. Lacoue-Nègre, J.-F. Joly, L. Duponchel, Low-Level Fusion of Fourier Transform Ion Cyclotron Resonance Mass Spectrometry Data Sets for the Characterization of Nitrogen and Sulfur Compounds in Vacuum Gas Oils, Analytical chemistry 92 (2020) 2815–2823.
[23] S. Bhosale, R. Manigiri, R.P. Choudhury, V. Bhakthavatsalam, High Resolution Mass Spectrometry and Principal Component Analysis for an Exhaustive Understanding of Acidic Species Composition in Vacuum Gas Oil Samples, Energy Fuels 34 (2020) 2800–2806.
[24] J. Guillemant, F. Albrieux, L.P. de Oliveira, M. Lacoue-Nègre, L. Duponchel, J.-F. Joly, Insights from Nitrogen Compounds in Gas Oils Highlighted by High-Resolution Fourier Transform Mass Spectrometry, Analytical chemistry 91 (2019) 12644–12652.
[25] A.N. Kozhinov, K.O. Zhurov, Y.O. Tsybin, Iterative method for mass spectra recalibration via empirical estimation of the mass calibration function for Fourier transform mass spectrometry-based petroleomics, Analytical chemistry 85 (2013) 6437–6445.
[26] U. Käfer, T. Gröger, C.P. Rüger, H. Czech, M. Saraji-Bozorgzad, T. Wilharm, R. Zimmermann, Direct inlet probe - High-resolution time-of-flight mass spectrometry as fast technique for the chemical description of complex high-boiling samples, Talanta 202 (2019) 308–316.
[27] E.M. Morales-Valencia, C.O. Castillo-Araiza, S.A. Giraldo, V.G. Baldovino-Medrano, Kinetic Assessment of the Simultaneous Hydrodesulfurization of Dibenzothiophene and the Hydrogenation of Diverse Polyaromatic Structures, ACS Catal. 8 (2018) 3926–3942.

6. Tables and Figures